Simultaneous bandgaps in LiNbO3 phoxonic crystal slab

Quentin Rolland,[1,*] Samuel Dupont,[1] Joseph Gazalet,[1] Jean-Claude Kastelik,[1] Yan Pennec,[2] Bahram Djafari-Rouhani,[2] and Vincent Laude[3]

[1]*Institut d'Electronique, de Micro-électronique et de Nanotechnologie, UMR CNRS 8520, Université de Valenciennes-Hainault-Cambrésis, Valenciennes, France*
[2]*Institut d'Electronique, de Micro-électronique et de Nanotechnologie, UMR CNRS 8520, UFR de Physique Université Lille 1, Villeneuve d'Ascq, France*
[3]*Institut FEMTO-ST, Université de Franche-Comté, CNRS, 32 Avenue de l'Observatoire, F-25044 Besançon Cedex, France*
[*]*quentin.rolland@univ-valenciennes.fr*

Abstract: We study simultaneous photonic and phononic crystal slabs created in Z-cut lithium niobate membranes. Bandgaps for guided waves are identified using the three-dimensional finite element method (FEM). Three lattices are considered: the square, the hexagonal, and the honeycomb lattices. We investigate the evolution of band gaps as a function of geometrical parameters such as hole radius and membrane thickness. We show the existence of dual photonic and phononic bandgaps in the triangular lattice for suitable geometrical parameters and specific modal symmetries for both the elastic and the electromagnetic fields.

OCIS codes: (160.5298) Photonic crystals; (160.1050) Acousto-optical materials; (230.1040) Acousto-optical devices; (350.7420) Waves.

References and links

1. E. Yablonovitch, "Inhibited Spontaneous Emission in Solid-State Physics and Electronics," Phys. Rev. Lett. **58**(20), 2059–2062 (1987).
2. J. D. Joannopoulos, S. G. Johnson, J. N. Winn, and R. D. Meade, Princeton University "Photonic crystals: Molding the Flow of Light," (2008).
3. M. S. Kushwaha, P. Halevi, L. Dobrzynski, and B. Djafari-Rouhani, "Acoustic band structure of periodic elastic composites," Phys. Rev. Lett. **71**(13), 2022–2025 (1993).
4. M. M. Sigalas and E. N. Economou, "Elastic and acoustic wave band structure," J. Sound Vibrat. **158**(2), 377–382 (1992).
5. Y. Pennec, J. Vasseur, B. Djafari-Rouhani, L. Dobrzynski, and P. A. Deymier, "Two-dimensional phononic crystals: Examples and applications," Surf. Sci. Rep. **65**(8), 229–291 (2010).
6. M. Maldovan and E. L. Thomas, "Simultaneous complete elastic and electromagnetic band gaps in periodic structures," Appl. Phys. B **83**(4), 595–600 (2006).
7. D. Bria, M. B. Assouar, M. Oudich, Y. Pennec, J. Vasseur, and B. Djafari-Rouhani, "Opening of simultaneous photonic and phononic band gap in two-dimentional square lattice periodic structure," Appl. Phys. (Berl.) **109**(1), 014507 (2011).
8. Y. Pennec, B. Djafari Rouhani, E. H. El Boudouti, C. Li, Y. El Hassouani, J. O. Vasseur, N. Papanikolaou, S. Benchabane, V. Laude, and A. Martinez, "Simultaneous existence of phononic and photonic band gaps in periodic crystal slabs," Opt. Express **18**(13), 14301–14310 (2010).
9. S. Mohammadi, A. A. Eftekhar, A. Khelif, and A. Adibi, "Simultaneous two-dimensional phononic and photonic band gaps in opto-mechanical crystal slabs," Opt. Express **18**(9), 9164–9172 (2010).
10. Y. El Hassouani, C. Li, Y. Pennec, E. H. El Boudouti, H. Larabi, A. Akjouj, O. Bou Matar, V. Laude, N. Papanikolaou, A. Martinez, and B. Djafari Rouhani, "Dual phononic and photonic band gaps in a periodic array of pillars deposited on a thin plate," Phys. Rev. B **82**(15), 155405 (2010).
11. Y. Pennec, B. Djafari Rouhani, C. Li, J. M. Escalante, A. Martinez, S. Benchabane, V. Laude, and N. Papanikolaou, "Band gaps and cavity modes in dual phononic and photonic strip waveguides," AIP Advances **1**(4), 041901 (2011).
12. A. Guarino, G. Poberaj, D. Rezzonico, R. Degl'Innocenti, and P. Günter, "Electro-optically tunable microring resonators in lithium niobate,"," Nat. Photonics **1**(7), 407–410 (2007).
13. N. Courjal, S. Benchabane, J. Dahdah, G. Ulliac, Y. Gruson, and V. Laude, "Acousto-optically tunable lithium niobate photonic crystal," Appl. Phys. Lett. **96**(13), 131103 (2010).
14. S. Sadat-Saleh, S. Benchabane, F. Issam Baida, M. P. Bernal, and V. Laude, "Tailoring simultaneous photonic and phononic band gaps," J. Appl. Phys. **106**(7), 074912 (2009).

#205728 - $15.00 USD Received 29 Jan 2014; revised 17 Mar 2014; accepted 27 Mar 2014; published 24 Jun 2014

15. D. Yudistira, Y. Pennec, B. Djafari Rouhani, S. Dupont, and V. Laude, "Non-radiative complete surface acoustic wave bandgap for finite-depth holey phononic crystal in lithium niobate," Appl. Phys. Lett. **100**(6), 061912 (2012).
16. A. Khelif, Y. Achaoui, S. Benchabane, V. Laude, and B. Aoubiza, "Locally resonant surface acoustic wave band gaps in a two-dimensional phononic crystal of pillars on a surface," Phys. Rev. B **81**(21), 214303 (2010).
17. Y. Achaoui, A. Khelif, S. Benchabane, L. Robert, and V. Laude, "Experimental observation of locally-resonant and Bragg band gaps for surface guided waves in a phononic crystal of pillars," Phys. Rev. B **83**(10), 104201 (2011).
18. G. W. Burr, S. Diziain, and M.-P. Bernal, "The impact of finite-depth cylindrical and conical holes in lithium niobate photonic crystals," Opt. Express **16**(9), 6302–6316 (2008).
19. F. Schrempel, T. Gischkat, H. Hartung, T. Höche, E.-B. Kley, A. Tünnermann, and W. Wesch, "Ultrathin membranes in x-cut lithium niobate," Opt. Lett. **34**(9), 1426–1428 (2009).
20. H. Hartung, E.-B. Kley, T. Gischkat, F. Schrempel, W. Wesch, and A. Tünnermann, "Ultra thin high index contrast photonic crystal slabs in lithium niobate," Opt. Mater. **33**(1), 19–21 (2010).
21. R. Geiss, S. Diziain, R. Iliew, C. Etrich, H. Hartung, N. Janunts, F. Schrempel, F. Lederer, T. Pertsch, and E.-B. Kley, "Light propagation in a free-standing lithium niobate photonic crystal waveguide," Appl. Phys. Lett. **97**(13), 131109 (2010).
22. S. Diziain, R. Geiss, M. Zilk, F. Schrempel, E.-B. Kley, A. Tünnermann, and T. Pertsch, "Second harmonic generation in free-standing lithium niobate photonic crystal L3 cavity," Appl. Phys. Lett. **103**(5), 051117 (2013).
23. J. Deng, S. Hussain, V. Sudheer Kumar, W. Jia, C. Eng Png, L. Soon Thor, A. A. Bettiol, and A. J. Danner, "Modeling and experimental investigations of Fano resonances in free-standing LiNbO3 photonic crystal slabs (Fabrication)," Opt. Express **21**(3), 3243 (2013).
24. V. Laude, J. C. Beugnot, S. Benchabane, Y. Pennec, B. Djafari-Rouhani, N. Papanikolaou, J. M. Escalante, and A. Martinez, "Simultaneous guidance of slow photons and slow acoustic phonons in silicon phoxonic crystal slabs," Opt. Express **19**(10), 9690–9698 (2011).
25. J.-M. Lourtioz, "Les cristaux photoniques ou la lumière en cage," Hermès-Science (2003).
26. M. Jazbinsek and M. Zgonik, "Material tensor parameters of LiNbO3 relevant for electro- and elasto-optics," Appl. Phys. B **74**(4-5), 407–414 (2002).
27. R. S. Weis and T. K. Gaylord, "Lithium niobate: Summary of physical properties and crystal structure," Appl. Phys., A Mater. Sci. Process. **37**(4), 191–203 (1985).
28. S. Hemon, A. Akjouj, A. Soltani, Y. Pennec, Y. El Hassouani, A. Talbi, V. Mortet, and B. Djafari-Rouhani, "Hypersonic band gap in an AlN-TiN bilayer phononic crystal slab," Appl. Phys. Lett. **104**(6), 063101 (2014).
29. P. Geng, W. Zhang, H. Zhang, S. Zhang, J. Ruan, S. Wei, and X. Xue, "Design of Broadband Single-Polarization Single-Mode Photonic Crystal Fiber Based on Index-Matching Coupling," IEEE Photon. Technol. Lett. **24**(6), 452–454 (2012).
30. C. G. Bostan, P. Schiopu, and O. Mita, Proc. SPIE **7297**, 72971M (2009).

1. Introduction

An artificial periodic structure can exhibit omnidirectional bandgaps, i.e., frequency ranges inside which wave propagation is forbidden regardless the direction of propagation. They are referred to as complete bandgaps when they apply to all polarizations. This property has been studied both for photons [1, 2] and phonons [3–5], in the so-called photonic and phononic crystals. Periodic structures presenting simultaneously photonic and phononic complete bandgaps are called phoxonic crystals [6]. The design of such structures drives a growing interest since they provide promising means of controlling light and sound. Several combinations of materials and lattices have been studied in order to demonstrate the occurrence of simultaneous bandgaps.

Maldovan and Thomas [6] have demonstrated the possibility to obtain simultaneous bandgaps in a two-dimensional silicon infinite crystal with a square-lattice array of air holes. D. Bria et al. [7] further investigated the evolution of bandgaps with the size of the inclusions and their simultaneity for periodic structures based on silicon or sapphire. Three dimensional structures with a finite depth have also received a great deal of attention, in particular periodic structures formed in membranes. The simultaneity of both photonic and phononic bandgaps in silicon membranes has been proven recently by two different authors [8, 9]. Related studies have also been conducted on the complementary structure: periodic arrays of silicon pillars deposited on a silica substrate [10]. In addition, some papers have discussed the possibility of enhanced photon/phonon interaction in strip waveguides [11].

Lithium Niobate is an appealing material owing to its particularly high acousto-optic, electro-optic and piezoelectric properties. It offers ultrafast modulation because of high electro-optic coefficients, and wide intrinsic bandwidth [12]. This material has been widely used for various applications like electro-optic / acousto-optic modulators and tunable filters.

#205728 - $15.00 USD Received 29 Jan 2014; revised 17 Mar 2014; accepted 27 Mar 2014; published 24 Jun 2014

These properties allow one to design integrated optical modulators with direct acoustic wave generation using interdigitated transducer [13]. S. Sadat-Saleh et al. [14] have identified phoxonic complete bandgaps for in-plane propagation in two-dimensional Z-cut based structures (Z-axis normal to the plate), considering the cases of the square, the triangular, and the boron nitride lattices. They have also analyzed the bandgap evolution with respect to the filling factor. Semi-infinite structures supporting elastic guided wave propagation at the surface have also been considered. For phononic crystals, Yudistira et al. [15] have reported the possibility to confine surface acoustic waves on finite depth holes in honeycomb lattice; complete band gaps for surface acoustic waves is also possible in the case of arrays of pillars on a surface [16,17]. For photonic crystals, Burr et al. [18] have studied the confinement of electromagnetic waves within a shallow holes structure drilled on a semi-infinite substrate. They concluded that in order to avoid leakage to the substrate, high aspect ratio holes are required, which still represents a technological challenge that has not been circumvented in semi-infinite Lithium Niobate structures.

In 2009, the use of Lithium Niobate membranes was suggested in order to circumvent deep holes issues [19–21]: the experimental feasibility of a photonic crystal microstructure on a $LiNbO_3$ free standing membrane has been demonstrated using Ion Beam Enhance Etching (IBEE) technology. More recently, a L3 microcavity in Lithium Niobate membrane has been reported [22], it offers a remarkable opportunity for the realization of phoxonic devices. Finally, J. Dung et al. measured the optical transmission based on Fano resonances [23] in LiNbO3 photonic slabs. Because the refractive indices of LiNbO3 are significantly smaller than the refractive index of silicon (about 2.2 as compared to about 3.5), the occurrence of phoxonic bandgaps in LiNbO3 is still an open question. It is known that the conditions to obtain phoxonic bandgaps are quite different in slabs rather than in the 2D infinite structures [8]. Moreover, owing to the piezoelectric nature of LiNbO3, the conditions to obtain phononic bandgaps are more demanding; also considering the relatively low refractive index of the material, the occurrence of photonic band gaps requirements are more stringent [14], especially in the case of slabs considered here. Therefore, we present here a first study of phoxonic slabs in piezoelectric materials.

In this article, we report on the theoretical investigation of complete photonic and phononic bandgaps in LiNbO3 Z-cut crystal slabs. We examine the possibility of confining optic and acoustic waves in membranes with square, hexagonal and honeycomb micro-structured lattices. More precisely, our purpose is to determine suitable geometrical parameters that provide phoxonic bandgaps. We compute the optical and acoustic bandgap maps and identify the optimum couples of geometrical parameters (radius, thickness) for phoxonic devices. In order to relax constraints on the optimization process, the consideration of the symmetry of modes with respect to the mid-plane of the slab is found to be essential. Among the numerical methods that are available to compute photonic and phononic dispersion curves, we use the finite element method (FEM) that is well suited for mode analysis calculation. Also, the mesh layout adaptability, offered by this numerical method, is fully adapted to fit the rather complicated geometries we consider.

2. Model definition

Following the traditional procedure, we compute the dispersion curves considering one unit-cell complimented with Bloch-Floquet periodic boundary conditions applied to the lateral boundaries. Regarding the top and bottom slab boundary conditions, we have to distinguish the photonic and the phononic simulations: as elastic waves do not propagate in air, free boundary conditions are applied at the air/solid interfaces; in the case of photonic crystal, periodic conditions are applied on top of a thick air domain. Its height is chosen in order to trade-off between accuracy and computation time. In practice, a reasonable size for the air domain has to be found ensuring convergence of the computation of photonic modes confined in the slab. With regards to leaky modes in the light cone, the bottom and top air boundaries introduce spurious modes whose number increases with the air thickness [24]. To dissociate confined (guided) and leaky modes, we exploit the concept of the light cone defined from the

#205728 - $15.00 USD Received 29 Jan 2014; revised 17 Mar 2014; accepted 27 Mar 2014; published 24 Jun 2014

dispersion relation for light in vacuum, $\omega = c \cdot k$ with ω the angular frequency and k the wavenumber. With $k_{//}$ the wavevector component parallel to the slab/air interface, the inside of the light cone is defined by $\omega > c \cdot k_{//}$. Inside the light cone, the normal component $k_{\perp}$ in the air region is real-valued and the optical energy flux of modes is allowed to leak outside of the slab. Outside the light cone, $k_{\perp}$ in the air region becomes complex imaginary and light is confined inside the slab [25]. This last case corresponds to total internal reflection at the slab interfaces.

In this paper we use the material parameters of references [26, 27] and as indicated in [26] due to the anisotropic nature of lithium niobate, a special attention to the symmetry of the material is required. Indeed, the crystallographic symmetry of the host material may limit the overall symmetry of the phoxonic crystal. Consequently, the first Brillouin zone path along which the band structure is analyzed has to be adapted. In the case of Z-cut LiNbO3, however, the relevant slowness curves (illustrated in Fig. 1(a)) display symmetries of the square, the hexagonal, and the honeycomb lattice (depicted in Fig. 1(b)-1(d) respectively). As a consequence, one can compute phononic dispersion curves following the standard paths i.e., along the irreducible Brillouin zone. Explicitly, dispersion curves were computed using the standard unit-cells presented in Fig. 1 with dashed lines and following the irreducible Brillouin zone paths around the respective shaded areas of the square, the hexagonal, and the honeycomb lattices.

The choice of Z-cut lithium niobate leads to an isotropic-like optical character for wavevectors k laying in the (X,Y) plane. Indeed, modes polarized within the (X,Y) plane experience only the ordinary refractive index whilst modes polarized along the optical axis Z are subject to the extraordinary refractive index. As a consequence, the symmetry of photonic crystal structures in Z-cut $LiNbO_3$ is not altered by material anisotropy and the dispersion curves can be displayed along the irreducible Brillouin zones traditionally used for isotropic media.

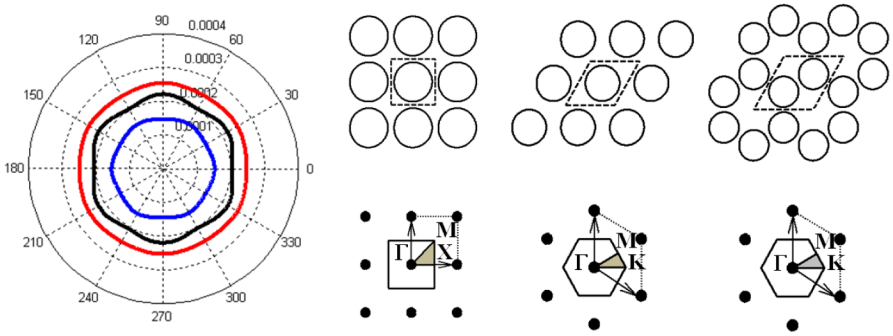

(a) (b) (c) (d)

Fig. 1. (a) Slowness curves of Z-cut LiNbO3. The blue, the black, and the red solid lines represent the longitudinal, the in-plane, and the out-of-plane shear inverse velocities, respectively. (b) Direct and reciprocal square lattice, and corresponding first irreducible Brillouin zone. The unit cell is represented with dashed line and the irreducible zone is shaded. (c) Triangular lattice and corresponding irreducible Brillouin zone. (d) Honeycomb lattice and corresponding irreducible Brillouin zone.

Likewise, one can take advantage of the symmetry of the geometrical structure and impose a symmetry plane midway along the membrane thickness. This allows to reduce the size of the model (save computer power and memory) and to separate the computation into even and odd modes for both photonic and phononic crystals.

#205728 - $15.00 USD Received 29 Jan 2014; revised 17 Mar 2014; accepted 27 Mar 2014; published 24 Jun 2014

3. Results and discussion

In what follows, we aim at determining photonic and phononic complete bandgaps for the square, the honeycomb, and the triangular lattices. The considered geometrical parameters are the inclusion radius *r*, the nearest neighbor distance a, and the membrane thickness h. Computations are performed on a suitable range of relative thicknesses *h/a* varying from *0.4* up to *0.8*, and for relative radius r/a varying from *0.25* up to *0.49*, leading to a reasonable set of graphs for a good overview of the evolution of bandgaps. Results are presented as a function of the acoustic and optical reduced frequencies $f \cdot a$ and $\omega \cdot a/2\pi \cdot c$ respectively, where c is the velocity of light in vacuum.

Figures 2, 3 and, 4 display the evolution of the bandgaps versus the ratio *r/a* for five relative thicknesses *h/a*. Figure 5 depicts a typical band structure, while Fig. 6 presents the results obtained for the corresponding 2D structures; it enables one to foresee the tendency when *h/a* tends towards infinity. In the following, we discuss the impact of the different lattices on the band structures and point out the occurrence of simultaneous acoustic and optic forbidden bands.

Figure 2 presents the projected bandgaps of a square lattice $LiNbO_3$ phoxonic crystal slab. Phononic and photonic bandgap evolutions are displayed on the top and the bottom of the figure, respectively. The unit-cell geometries are inserted on the bottom of each graph. The blue and the red colors indicate bandgaps for even and odd modes, respectively, for both photonic and phononic properties of the crystal; the pink color represents the complete bandgaps; the black horizontal solid lines represent the reduced frequencies (1/2 and $1/\sqrt{2}$) at the light cone X and M symmetry points respectively.

We can notice at first glance that even bandgaps are predominant in the phononic behavior of the structure and are relatively unaffected by the thickness parameter. Two odd bandgaps exist: the first one is situated around $f \cdot a = 2250$ for $h/a = 0.4$ and get thinner as the membrane thickness increases. The second one appears at higher frequency and gets wider as the membrane thickness increases. The anti-symmetric gap is more sensitive to the thickness of the plate because some of the dispersion curves of odd symmetry, which have a predominant out-of-plane vibration, are more sensitive to the thickness of the plate than other branches and define the position and width of the band gap [28]. For photonic modes, the even bandgaps are predominant too. The even and odd bandgaps get thinner and split in numerous bandgaps for higher membrane thicknesses. The even modes mid-gap frequencies are lowering down with increasing thickness. Only the lowest frequency band presents a non leaky omnidirectional character as it lies under the reduced frequency limit of 1/2.

Finally, for any given normalized radius r/a, there is no photonic and phononic bandgaps at the same time. The phononic bandgaps appear for the higher range of relative inclusions radius parameters, whereas the photonic bandgaps reach the upper limit for non leaky modes. This observation holds whatever the value of *h/a* is, although a dim coincidence of the bandgaps appears at $h/a = 0.7$. As a consequence, we can deduce that the square lattice does not allow simultaneous bandgaps for lithium niobate membranes.

#205728 - $15.00 USD Received 29 Jan 2014; revised 17 Mar 2014; accepted 27 Mar 2014; published 24 Jun 2014

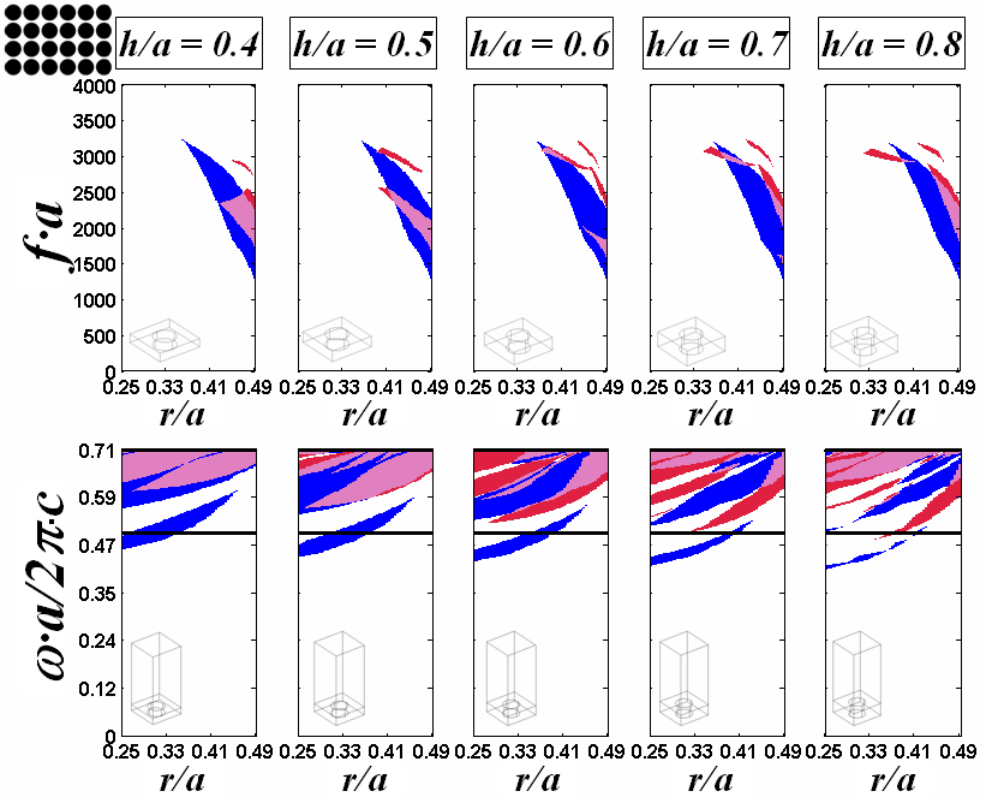

Fig. 2. Evolution of optical (bottom row) and acoustic (top row) bandgaps for the square lattice as a function of *r/a*, for different values of *h/a*; blue: symmetric (even) modes bandgaps, red anti-symmetric (odd) modes bandgaps, pink: complete bandgaps; black solid lines: reduced frequencies (1/2 and 1/√2) at the light cone X and M symmetry points respectively.

An analogous study was conducted for the honeycomb lattice. Figure 3 shows that the even phononic bandgap is predominant and is again practically not affected by the slab thickness ratio, similarly to the square lattice case. There is one unique odd bandgap which is slightly widening and rising up with the thickness. These gaps are wider than in the square lattice case.

Considering the photonic crystal behavior, the even bandgap is predominant. For both symmetries, mid-gap frequencies are dropping down for higher thicknesses; their lower limit reaches the normalized frequency value *0.33*, which corresponds to the upper limit for a non leaky omnidirectional gap for the honeycomb lattice. Only a few non leaky modes exist for geometrical parameters where the phononic bandgaps are too thin to be exploitable thus no simultaneous bandgaps appear.

#205728 - $15.00 USD Received 29 Jan 2014; revised 17 Mar 2014; accepted 27 Mar 2014; published 24 Jun 2014

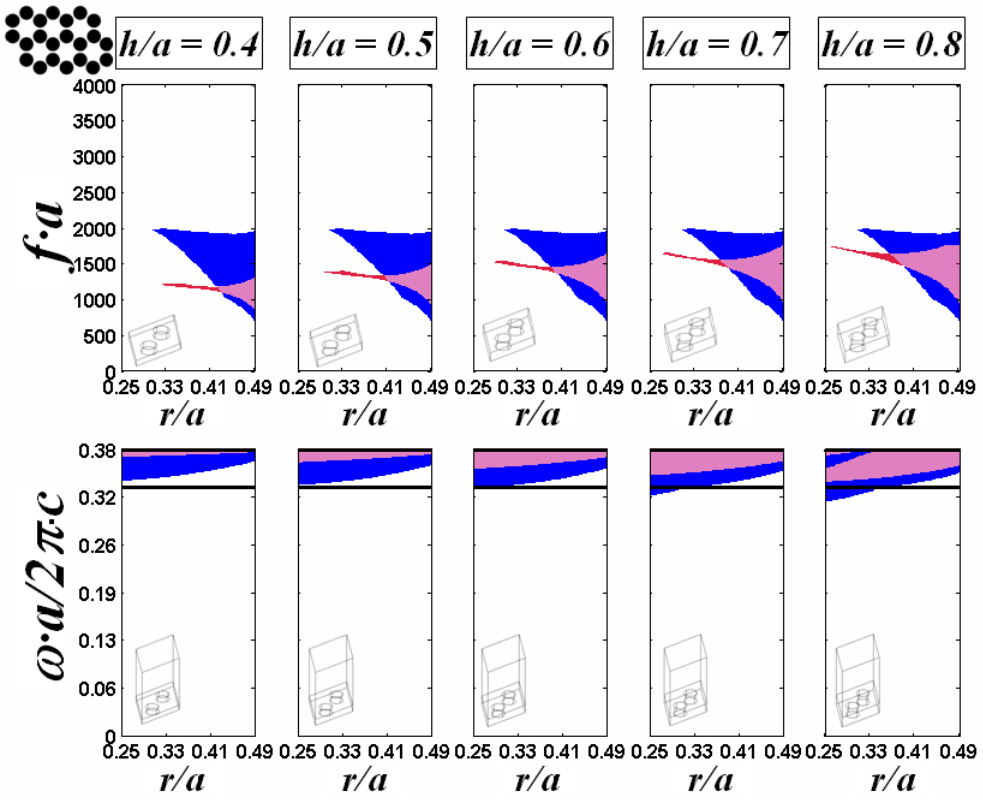

Fig. 3. Evolution of optical (bottom row) and acoustic (top row) bandgaps for the honeycomb lattice as a function of *r/a*, for different values of *h/a*; blue: symmetric (even) modes bandgaps, red anti-symmetric (odd) modes bandgaps, pink: complete bandgaps; black solid lines: reduced frequencies (1/3 and 2/3√3) at the light cone M and K symmetry points respectively.

Finally, the triangular (hexagonal) lattice results are presented in Fig. 4. As compared to the square and the honeycomb lattices, the structure presents thinner phononic bandgaps which can be differentiated into thin and moderately thick bandgaps. The thin ones are very narrow and are located around $f{\cdot}a = 1000$ and $f{\cdot}a = 3000$ for the even and odd modes respectively, yet they are too thin to be good candidates for acoustical confinement. The thicker ones are odd bandgaps, they appear for $f{\cdot}a = 3000$ for a low radius up to a thickness ratio *h*/a of *0.6*. However, these bandgaps show a non-continuous behavior with increasing thicknesses: the moderate bandgaps vanish for reduced thickness higher than *0.6*.

As before, there is a predominance of the even photonic bandgaps. Both odd and even bandgap frequencies are lowering down as the membrane thickness increases. Bandgaps, especially the odd ones, split with growing membrane thicknesses. One can notice that one even bandgap is under the reduced frequency of $1/\sqrt{3}$ which corresponds to the non leaky omnidirectional gap upper frequency limit. Hence, the hexagonal lattice presents photonic bandgaps which extend over a large range of geometrical parameters.

This allows designing a phoxonic structure which takes advantage of the moderately thick phononic odd bandgaps. For instance, the normalized radius range [*0.25-0.33*] and the normalized thickness $h/a = 0.6$ give simultaneous bandgaps for odd phononic and even photonic modes. As an illustrative example, we present in Fig. 5 the dispersion curves corresponding to the *r/a* value of 0.28 which gives an appreciable bandwidth for both waves: a phononic fractional bandwidth of 9.21% centered at the reduced frequency $f.a = 2811$ *m/s*, together with a photonic fractional bandwidth of 11.8% centered at an optical reduced frequency of 0.4021. Assuming the telecommunication wavelength of *1550 nm*, the geometrical parameters are: $a = 623$ *nm*, $h = 374$ *nm*, and $r = 174.5$ *nm*. The corresponding

#205728 - $15.00 USD Received 29 Jan 2014; revised 17 Mar 2014; accepted 27 Mar 2014; published 24 Jun 2014

acoustic frequency is 4.51 GHz. These parameters are in good agreement with technological feasibility. Polarization dependent structures are still of interest, for polarization purpose as an example [29,30].

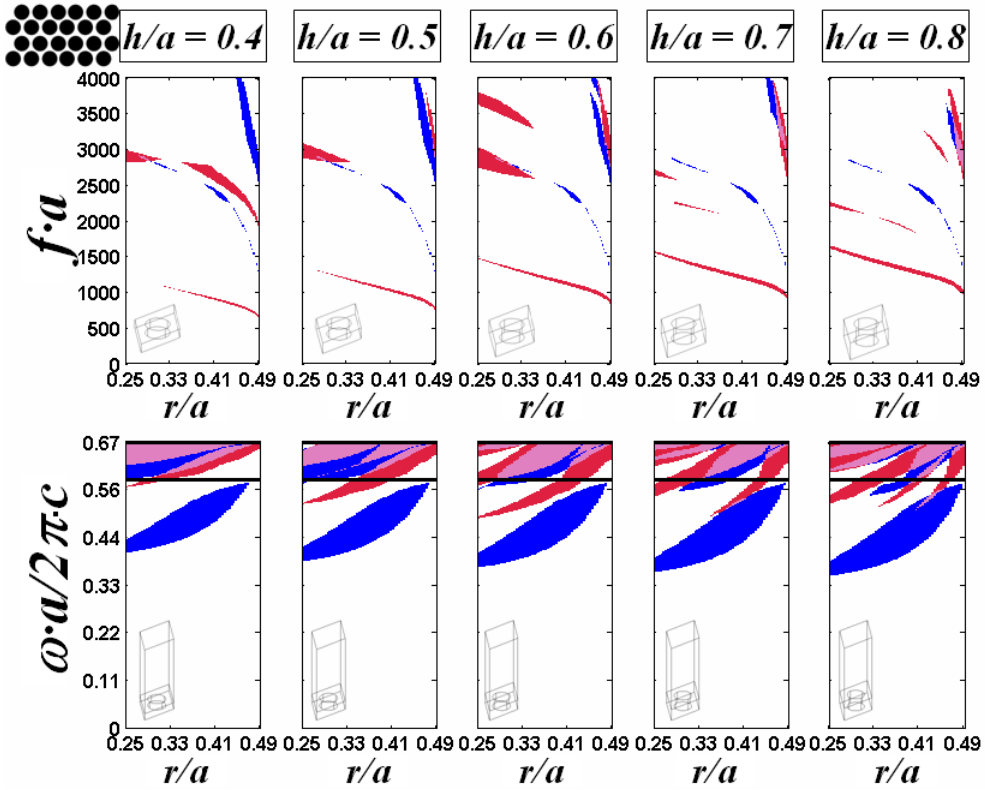

Fig. 4. Evolution of optical (bottom row) and acoustic (top row) bandgaps for the triangular lattice as a function of *r/a*, for different values of *h/a*; blue: symmetric (even) modes bandgaps, red anti-symmetric (odd) modes bandgaps, pink: complete bandgaps; black solid lines: reduced frequencies ($1/\sqrt{3}$ and 2/3) at the light cone M and K symmetry points respectively.

#205728 - $15.00 USD Received 29 Jan 2014; revised 17 Mar 2014; accepted 27 Mar 2014; published 24 Jun 2014

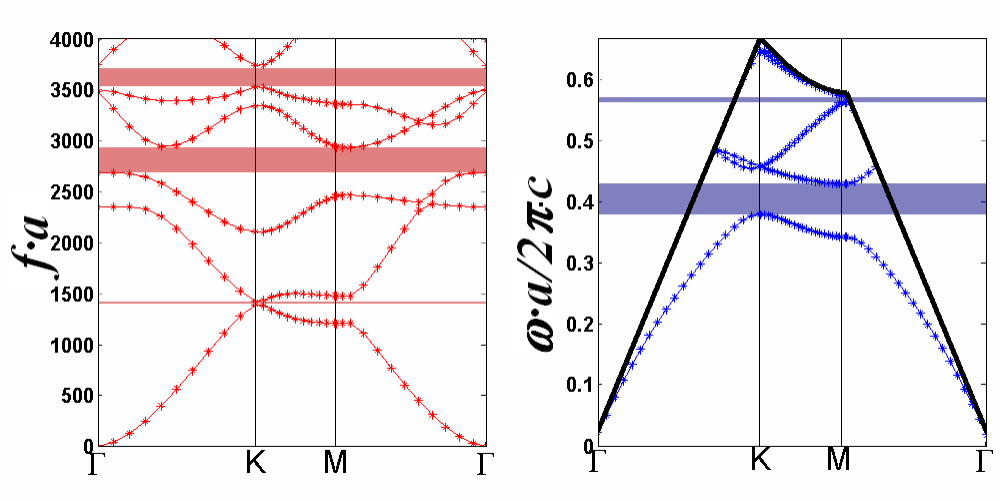

Fig. 5. Band structure for the triangular lattice for r/a = 0.28, for different values of h/a = 0.6. Left: anti-symmetric phononic modes; right symmetric photonic modes, the solid line represents the light cone.

Figure 6 represents the evolution of 2D infinite phononic bandgaps as a function of the normalized radius for the square lattice (Fig. 6(a)), the honeycomb lattice (Fig. 6(b)), and the hexagonal lattice (Fig. 6(c)). The blue and red bandgaps are the in-plane and out-of-plane bandgaps. As compared to slab (3D) calculations, we can notice a similar shape between the 2D in-plane bandgaps and 3D even phononic bandgaps for all lattices. Even bandgap reduced frequencies are relatively constant with respect to the membrane thickness. In contrast, the behavior of the 3D odd bandgap and the out-of-plane 2D bandgaps are quite dissimilar. The computed 3D odd bandgaps are thinner than even bandgaps and are strongly dependent on the membrane thickness.

Furthermore, by direct comparison with reference [14], optical bandgaps computed for the 2D model confirm the tendency observed with 3D computations when the thickness is increased, especially for the hexagonal lattice.

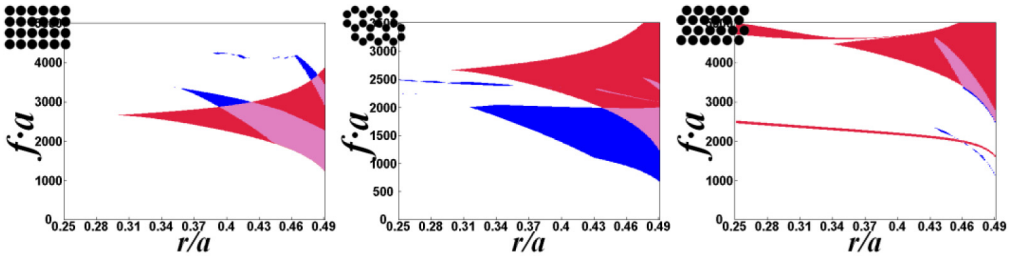

Fig. 6. Evolution of acoustic bandgaps for the square (a), the honeycomb (b), and the hexagonal (c) lattices as a function of the normalized radius. The blue, the red and the pink colour bandgaps represent the in-plane polarisation, the out-of-plane polarization and the complete bandgaps respectively.

4. Conclusion

The opening of simultaneous photonic and phononic bandgaps in lithium niobate slabs has been theoretically studied using the finite element method. The square, the triangular and the honeycomb lattices have been investigated for a set of geometrical parameters ranging from *0.4* to *0.8* for the relative slab thickness and from *0.25* to *0.5* for the air inclusion relative radius. The square lattice presents moderate bandgaps for photons and phonons but no

#205728 - $15.00 USD Received 29 Jan 2014; revised 17 Mar 2014; accepted 27 Mar 2014; published 24 Jun 2014

convincing coincidence is found with respect to the geometrical parameters. The honeycomb lattice appears to be the one auguring the wider phononic bandgaps, although no omnidirectional photonic bandgap is found outside the light cone. Finally, it is found that the hexagonal (or triangular) lattice supports phoxonic bandgaps: it promotes simultaneously the widest photonic bandgaps for the even modes and provide at the same time odd phononic bandgaps. The geometrical parameters are identified around reduced thickness of *0.6* and reduced inclusion radius of *0.3*; considering telecommunication optical wavelength, the phonon frequencies fall in the GHz range.

These outcomes will promote the design of phoxonic $LiNbO_3$ slab devices for experimental investigations.

#205728 - $15.00 USD Received 29 Jan 2014; revised 17 Mar 2014; accepted 27 Mar 2014; published 24 Jun 2014